ResearchGate

See discussions, stats, and author profiles for this publication at: https://www.researchgate.net/publication/229308326

Stability and structural features of DNA intercalation with ethidium bromide, acridine orange and methylene blue

ARTICLE *in* JOURNAL OF MOLECULAR STRUCTURE · FEBRUARY 2007

Impact Factor: 1.6 · DOI: 10.1016/j.molstruc.2006.05.004

CITATIONS
156

READS
437

5 AUTHORS, INCLUDING:

Shohreh Nafisi
Nanodermatology Research Group, IAUCTB…
64 PUBLICATIONS **831** CITATIONS
SEE PROFILE

Ali Akbar Saboury
University of Tehran
384 PUBLICATIONS **3,904** CITATIONS
SEE PROFILE

Heidar-Ali Tajmir-Riahi
Université du Québec à Trois-Rivières
261 PUBLICATIONS **6,598** CITATIONS
SEE PROFILE

Available from: Heidar-Ali Tajmir-Riahi
Retrieved on: 25 January 2016

Available online at www.sciencedirect.com
SCIENCE DIRECT®
Journal of Molecular Structure xxx (2006) xxx–xxx
Journal of MOLECULAR STRUCTURE
www.elsevier.com/locate/molstruc

Stability and structural features of DNA intercalation with ethidium bromide, acridine orange and methylene blue

Shohreh Nafisi [a,*], Ali Akbar Saboury [b], Nahid Keramat [a], Jean-Francois Neault [c], Heidar-Ali Tajmir-Riahi [c]

[a] Deparment of Chemistry, Azad University, Central Tehran Branch, 14169 63316 Tehran, Iran
[b] Institute of Biochemistry and Biophysics, University of Tehran, Tehran, Iran
[c] Department of Chemistry and Biology, University of Quebec at Trois-Rivieres, C.P. 500, TR, Que., Canada G9A 5H7

Received 1 March 2006; received in revised form 27 April 2006; accepted 2 May 2006

Abstract

Ethidium bromide (EB), acridine orange (AO), methylene blue (MB) and other fluorescent compounds are often used to probe DNA structure in drug–DNA and protein–DNA interactions. They bind nucleic acids via intercalative mode and cause major changes to DNA and RNA structures. The aim of this study was to examine the stability and structural features of calf-thymus DNA complexes with EB, AO and MB in aqueous solution, using constant DNA concentration (12.5 mM) and various pigment/DNA(P) ratios of 1/40, 1/20, 1/10, 1/4 and 1/2. FTIR, UV–visible spectroscopy and isothermal titration calorimetry (ITC) are used to determine the ligand intercalation and external binding modes, the binding constant and the stability of pigment–DNA complexes in aqueous solution. Structural analysis showed major intercalation of EB, AO and MB into polynucleotides G–C and A–T base pairs with minor external binding and overall binding constants of $K_{EB} = 6.58 \times 10^4$ M^{-1}, $K_{AO} = 2.69 \times 10^4$ M^{-1} and $K_{MB} = 2.13 \times 10^4$ M^{-1}. The overall binding constants estimated by UV–visible spectroscopy are consistent with thermodynamic data obtained by ITC, which showed $\Delta H(EB) = -13.58$ kJ/mol, $\Delta H(AO) = -14.63$ kJ/mol and $\Delta H(MB) = -13.87$ kJ/mol with dissociation constants of $K_{EB} = 15$ μM, $K_{AO} = 36$ μM and $K_{MB} = 46$ μM.
© 2006 Elsevier B.V. All rights reserved.

Keywords: DNA; Ethidium bromide; Acridine orange; Methylene blue; Binding constant; Binding mode; Conformation; Stability; Secondary structure; FTIR; UV–visible spectroscopy; Titration calorimetry

1. Introduction

Ethidium bromide [(3,8-diamino-5-ethyl-6-phenyl phenanthridinium bromide)], acridine orange [3,6-bis(dimethyl)acridinium chloride hemi(zinc chloride salt)], methylene blue [3,7-bis(dimethylamino)pheno-thrazin-5-ium chloride] and similar fluorescent compounds are normally used to probe DNA structure in drug–DNA and protein–DNA interactions [1]. They bind DNA and RNA via intercalative mode and slip between adjacent base pairs and cause stretch of double helical structure [1–7]. The binding of these pigments to double-stranded DNA greatly enhances its fluorescence intensity and lifetime [8–11] and inhibits a wide range of biologically important processes, such as DNA synthesis and gene transcription and translation [12,13]. It has been reported that EB shows significant antitumor [14,15] and anti-viral properties [16,17]. These activities are consequence of high affinity of ethidium for DNA duplex [18–22]. The pigment base stacking propensity and intercalation site specificity depend upon electrostatic interactions [23,24]. Electrostatic complementation is an important factor in π-stacking interactions [25–27]. Most carbon and hydrogen atoms in dye have relatively high electron densities and will exhibit energetically favorable π-stacking interactions with nucleobase pairs [25,26,28,29]. The partial positive charge on ethidium exocyclic amines is important for mediating electrostatic attraction and hydrogen bonding interactions with DNA phosphate groups and may strengthen their hydrogen bonding with DNA phosphate

* Corresponding author.
E-mail address: drshohreh@yahoo.com (S. Nafisi).

0022-2860/$ - see front matter © 2006 Elsevier B.V. All rights reserved.
doi:10.1016/j.molstruc.2006.05.004

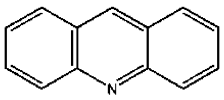

Acridine Orange

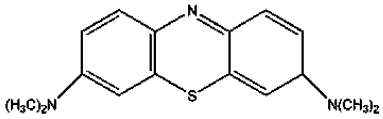

Methylene Blue

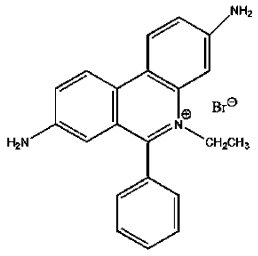

Ethidium Bromide

groups [2]. The phosphate and amino groups are within hydrogen bonding distances in a crystal structure of ethidium intercalated into nucleotide diphosphates [2].

Methylene blue is the most widely used photosensitizing agent and alternative to ethidium bromide. The exact mode of binding of MB to DNA duplex is unknown but its ionic interaction with negatively charged backbone PO_2 groups can cause photo-oxidative damages generating singlet oxygen through a triplet–triplet energy transfer from the photoexcited dye to molecular oxygen [30,31]. In case of MB binding to DNA with alternating G–C base sequence, the spectroscopic data clearly indicated intercalation of the planar heterocyclic MB between neighboring base pairs [32–35], whereas in the case of binding to DNA with alternating base sequences, minor groove binding is assumed to be the predominant binding mode [32,35–38]. The planar heterocyclic dye is expected to stabilize its binding to DNA through favorable stacking interactions with its adjacent base pairs [30].

Acridine orange has also been used as a fluorescent agent for nucleic acids in agarose and polyacrylamide gels. It has been used extensively for cell staining of DNA in apoptosis studies. It binds DNA via intercalation and stabilizes pigment–DNA complexes through charge neutralization of DNA backbone phosphate group.

We now report the results of our study on the structural analysis of EB, AO and MB complexes with calf-thymus DNA in aqueous solution, using FTIR, UV–visible spectroscopic methods and microcalorimetric measurements. The pigment intercalation and external binding with DNA duplex have been discussed and the stability of dye–DNA complexes formed is reported here.

2. Methods and materials

2.1. Materials

Highly polymerized type I calf-thymus DNA sodium salt (7% Na content) was purchased from Sigma Chemical Co. and was deproteinated by the addition of $CHCl_3$ and isoamyl alcohol in NaCl solution. Acridine orange, methylene blue and ethidium bromide were obtained from Merck Co. and used as supplied. Other chemicals were of reagent grade and used without further purification.

2.2. Preparation of stock solutions

Na-DNA was dissolved to 0.5% w/w, (12.5 mM DNA/phosphate) in 0.1 M NaCl and 1 mM sodium cocodylate (pH 7.30) at 5 °C for 24 h with occasional stirring to ensure formation of homogeneous solution. The solutions of acridine orange, methylene blue and ethidium bromide at different concentrations (2.5, 1.25, 0.625, 0.312 mM) were also prepared. Mixtures of drug and DNA were prepared by adding acridine orange, methylene blue or ethidium bromide dropwise to the DNA solution with constant stirring to give the desired drug/DNA molar ratios of 1/40, 1/20, 1/10, 1/4 and 1/2 at a final DNA concentration of 0.25% w/w or 6.25 mM DNA. Solution pH was adjusted between 6 and 7 with NaOH solution (0.1 M). The IR spectra were recorded 3 h after initial mixing of drug and DNA solutions.

2.3. Absorption spectroscopy

The absorption spectra were recorded on a LKB model 4054 UV–vis spectrometer, using various pigment concentrations (5 μM to 0.05 mM) and DNA concentration of 0.1 mM.

2.4. FTIR spectroscopic measurements

Infrared spectra were recorded on a BOMEM-DA3 with a HgCdTe detector and KBr beam splitter. Solution spectra were taken using AgBr windows with resolution of 4 cm^{-1} and 100 scans. Each set of infrared spectra was taken (three times). The water subtraction was carried out with 0.1 mM NaCl solution used as a reference at pH 6.5–7.5 [39]. A good subtraction was achieved as shown by a flat baseline around 2200 cm^{-1} where the water combination mode is located. The spectra were analyzed with OMNIC software. The FTIR difference spectra [(DNA solution + pigment solution) − (DNA solution)] were produced, using the band at 968 cm^{-1} as internal reference. This band is due to the sugar C–C stretching modes and shows no spectral changes upon dye complexation. The intensity ratio variations of several DNA in-plane vibrations related to A–T and G–C base pairs as well as the backbone PO_2 stretching were measured with respect to the reference band at 968 cm^{-1} as a function of drug concentrations with an error of ±3%. These intensity ratios were used to determine drug binding to DNA bases or the backbone phosphate groups [40–45].

2.5. Isothermal titration calorimetry

The isothermal titration microcalorimetric experiments were performed with Thermal Activity Monitor 2277, Thermometric, Sweden. Ligand solution (30 mM) was injected by use of a Hamilton syringe into the calorimetric stirred

titration stainless steel vessel, which contained 1.8 ml DNA (50 μM). The injection volume in each step was 10 μL. Thin (0.15 mm inner diameter) stainless steel hypodermic needles, permanently fixed to the syringe, reached directly into the calorimetric vessel. The calorimetric signal was measured by a digital voltmeter that was part of a computerized recording system. The heat of each injection was calculated by the ''Thermometric Digitam 3'' software program. The heat of dilution of the ligand solution was measured as described above except that DNA was excluded. Also, the heat of dilution of DNA solution was measured as described above except the buffer solution was injected to the DNA solution in the sample cell. The enthalpies of dilution for ligand and DNA solutions were subtracted from the enthalpy of DNA–ligand interaction. The microcalorimeter was frequently calibrated electrically during the course of the study.

3. Results and discussion

3.1. FTIR spectra

To examine the interaction of calf-thymus DNA with pigments, the infrared spectra of DNA and its dye complexes with various molar ratios of the dye/DNA (phosphate) were recorded. Evidence for pigment–DNA complexation comes from the infrared spectroscopic results shown in Figs. 1–3.

3.2. Methylene blue–DNA adduct

The spectral changes (intensity and shifting) of several prominent DNA in-plane vibrations at 1717 cm^{-1} (G, T), 1663 cm^{-1} (T, G, A and C), 1609 cm^{-1} (A, C), 1492 cm^{-1} (C, G) and 1222 cm^{-1} (PO_2 asymmetric stretch) [39–49]

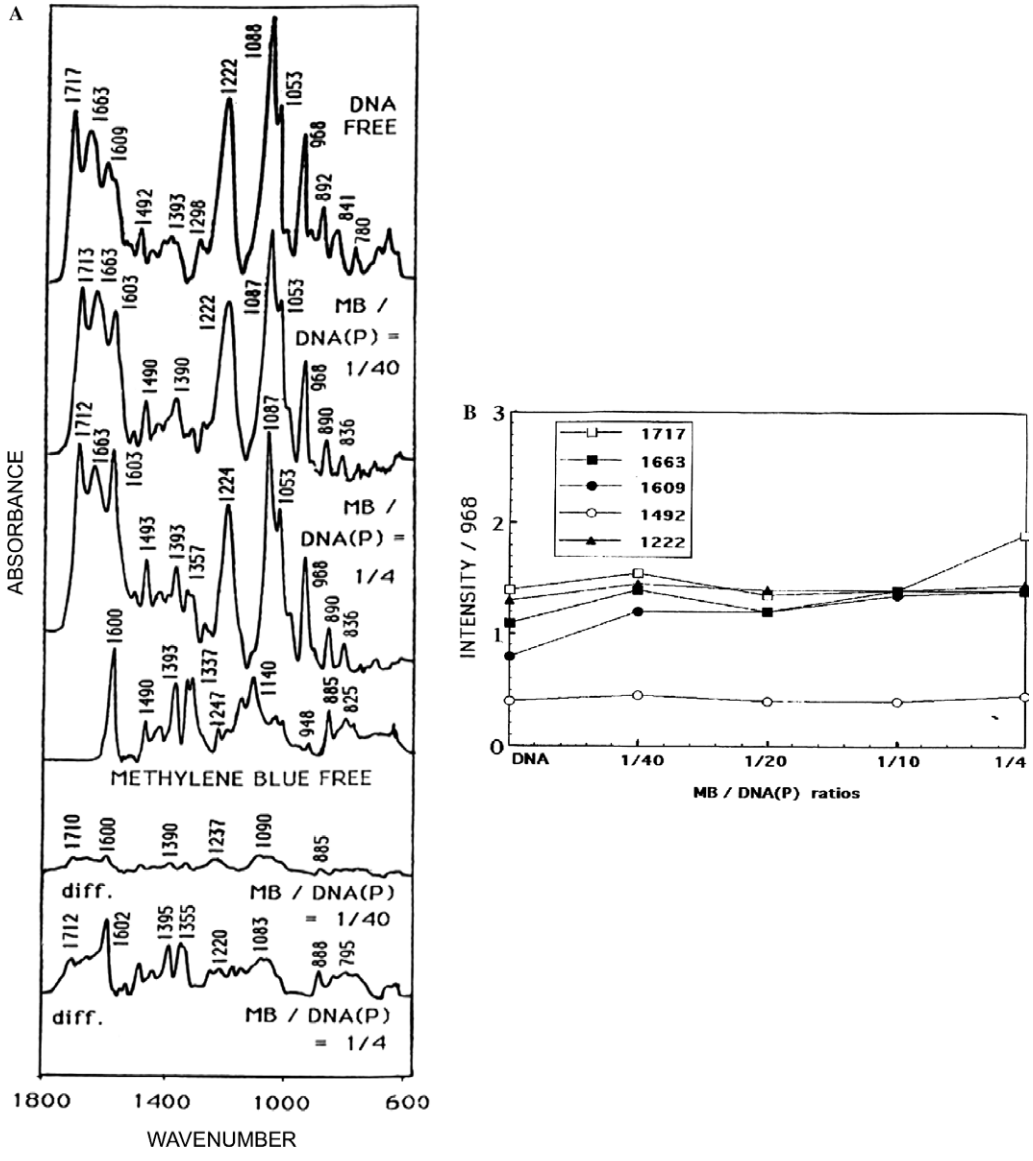

Fig. 1. (A) FTIR spectra and different spectra of calf-thymus DNA and its complexes with methylene blue (MB) in the region of 1800–600 cm^{-1} at different pigment/DNA(P) molar ratios and (B) the intensity ratio variations for several DNA vibrations 1717 (G), 1663 (T), 1609 (A), 1492 (C and G) and 1222 cm^{-1} (PO_2 stretch) as a function of pigment concentrations.

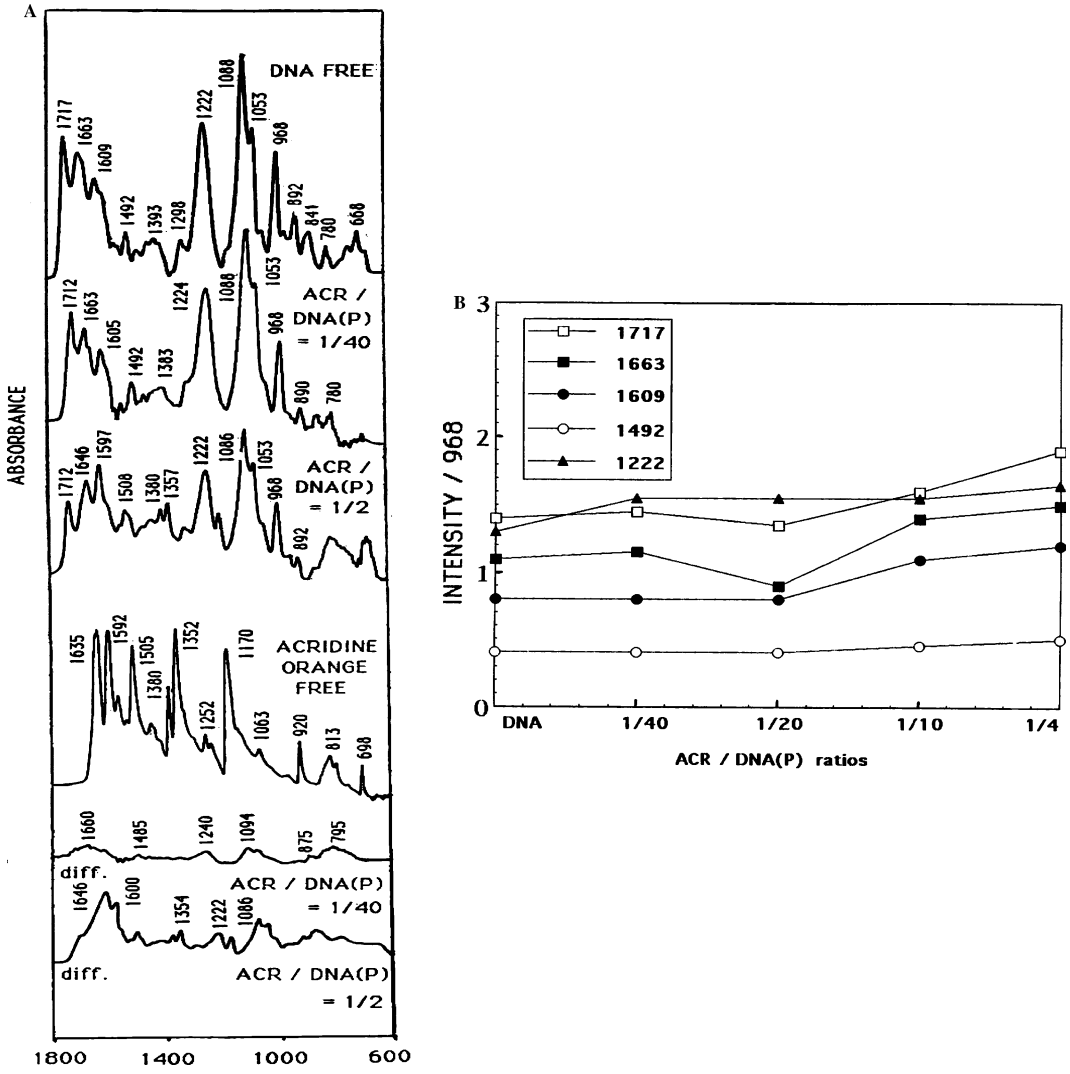

Fig. 2. (A) FTIR spectra and different spectra of calf-thymus DNA and its complexes with acridine orange (AO) in the region of 1800–600 cm^{-1} at different pigment/DNA(P) molar ratios and (B) The intensity ratio variations for several DNA vibrations 1717 (G), 1663 (T), 1609 (A), 1492 (C and G) and 1222 cm^{-1} (PO_2 stretch) as a function of pigment concentrations.

were monitored at different dye–DNA molar ratios and the results are shown in Fig. 1. Evidence for MB intercalation into DNA base pairs comes from minor intensity increase of DNA in-plane vibrations at 1717 (G), 1663 (T), 1609 (A), and 1222 cm^{-1} (PO_2 asymmetric stretch) upon pigment interaction (Fig. 1A and B). The major shifting of the band at 1717 (G) to 1713 cm^{-1} is indicative of dye intercalation mainly into the G–C base pairs (Fig. 1A). However, the thymine band at 1663 cm^{-1} exhibited no shifting upon dye complexation. The adenine band at 1609 cm^{-1} was overlapped with strong pigment absorption band at 1600 cm^{-1}, which makes it difficult to draw a certain conclusion on the nature of dye interaction with A–T bases (Fig. 1A). At high MB concentrations $r > 1/10$, a major increase in intensity of guanine band at 1717 cm^{-1} was observed with the shifting of this vibration to 1712 cm^{-1}, which is indicative of some degree of MB external binding to guanine bases (Fig. 1A). However, the shifting of the PO_2 asymmetric band at 1222–1224 cm^{-1} with some increase in intensity of this vibration is due to MB interaction with the backbone PO_2 groups (Fig. 1A and B).

3.3. Acridine orange–DNA adduct

Evidence for intercalation of acridine orange into DNA base pairs comes from minor intensity increase of DNA vibrations at 1717 (G) and 1222 cm^{-1} (PO_2 stretch) upon dye complexation (Fig. 2A and B). The increase in intensity of the band at 1717 cm^{-1} was associated with a major shifting of this band towards lower frequency at 1712 cm^{-1}. The spectral changes (intensity and shifting) guanine band at 1717 cm^{-1} are indicative of AO intercalation mainly to the G–C base pairs, while the major intensity increase of the phosphate band at 1222 cm^{-1} can be due to AO–PO_2 interaction (externally). However, due to overlapping of the thymine band at 1663 and adenine band at 1609 cm^{-1} with pigment vibrations, it was

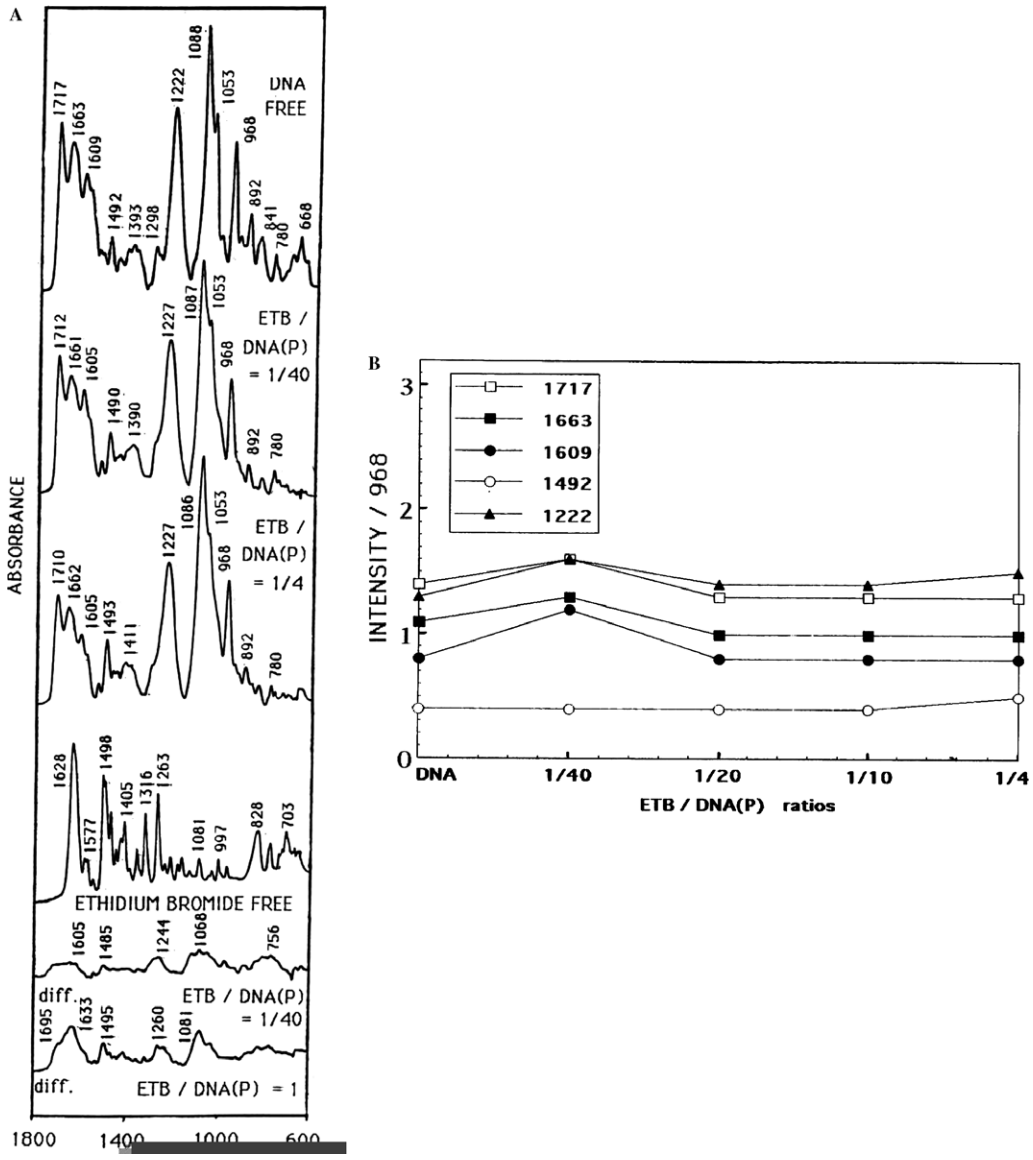

Fig. 3. (A) FTIR spectra and different spectra of calf-thymus DNA and its complexes with ethidium bromide (EB) in the region of 1800–600 cm^{-1} at different pigment/DNA(P) molar ratios and (B) The intensity ratio variations for several DNA vibrations 1717 (G), 1663 (T), 1609 (A), 1492 (C and G) and 1222 cm^{-1} (PO_2 stretch) as a function of pigment concentrations.

difficult to draw a certain conclusion on the pigment binding to A–T bases (Fig. 2A). At high AO concentrations $r > 1/10$, a major increase in intensity of the guanine band at 1717 $cm^{-1}$was observed which is indicative of some degree of AO external binding to guanine bases (Fig. 2B).

3.4. Ethidium bromide–DNA adduct

EB is a strong DNA binder and has been widely used to probe DNA structure upon drug or protein interaction. Evidence for EB intercalation comes from major intensity increase for DNA in-plane vibrations at 1717 (G), 1663 (T), 1609 (A) and the PO_2 band at 1222 cm^{-1} upon pigment adduct formation (Fig. 3A and B). The increase in intensity of these vibrations together with major shifting of the guanine band at 1717–1712, thymine band at 1663–1662 and adenine band at 1609–1605 cm^{-1} are due to EB intercalation into the G–C and A–T base pairs (Fig. 3A and B). On the other hand, the major intensity increase of the phosphate band at 1222 and the shifting to 1227 cm^{-1} are related to the EB–PO_2 interaction (external binding). It is important to note that the pigment–PO_2 binding continues even at high EB concentrations ($r = 1/4$), due to the major intensity increase of the backbone PO_2 band at 1222 cm^{-1} (Fig. 3B).

3.5. DNA conformation

A partial B to A transition occurred upon pigment complexation. Evidence for this comes from the shift of DNA marker infrared bands for the guanine at 1717 (G) to

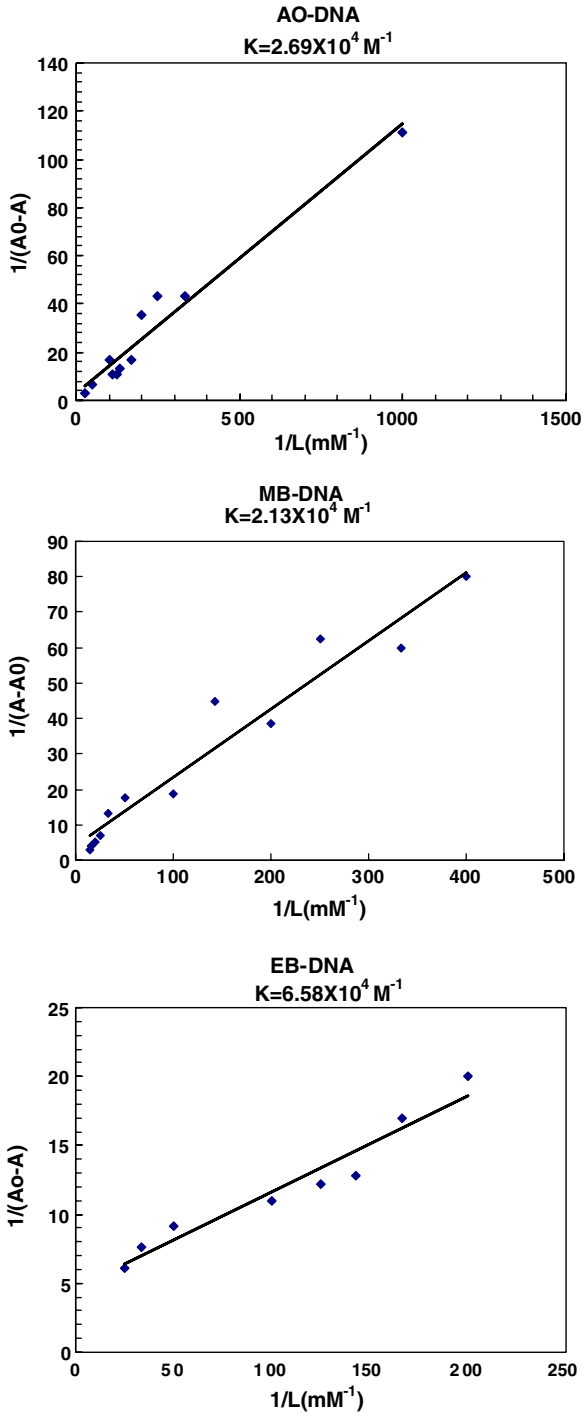

Fig. 4. The plot of $1/(A_0 - A)$ vs. 1/pigment concentration for DNA and their dye complexes where A_0 is the initial absorption of DNA (260 nm) and A is the recorded absorption at different pigment concentrations (L).

1713–1710 cm^{-1}, the phosphate at 1222 to 1227–1224 cm^{-1} and the phosphate-ribose diester linkage at 841 to 836–835 cm^{-1} in the spectra of pigment–DNA complexes (Figs. 1A, 2A and 3A). In a B to A transition, the band at 836 appears at about 820–810 cm^{-1}, while the PO_2 stretching vibration at 1222 shifts towards a higher frequency at 1240 cm^{-1} and the guanine band at 1717 appears at 1700 cm^{-1} [46–48]. The spectral changes observed for the DNA marker bands are due to a partial B to A transition upon MB, AO and EB interactions (Figs. 1A, 2A and 3A).

3.6. Absorption spectra of methylene blue, acridine orange, ethidium bromide–DNA complexes

3.6.1. Stability of pigment–DNA adducts

The calculation of the overall binding constants was carried out using UV spectroscopy as reported [49–53]. If the equilibrium for each drug with DNA were established as

$$\text{Drug} + \text{DNA} \Longleftrightarrow \text{Drug} : \text{DNA}$$

$$K = \frac{[\text{Drug} : \text{DNA}]}{[\text{Drug}][\text{DNA}]}$$

The double reciprocal plot of 1/[drug complexed] vs. 1/[drug] is linear and the association binding constant (K) is calculated from the ratio of the intercept on the vertical coordinate axis to the slope [50–53] (Fig. 4). Concentrations of complexed drug were determined by subtracting absorbance of uncomplexed DNA at 260 nm from that of the complexed DNA. Concentrations of drugs were determined by subtraction of complexed drug from total drug used for the experiment. Our data of 1/[drug complexed] almost proportionally increased as a function of 1/[free drug] (Fig. 4), and thus, the overall binding constants are estimated to be K(methylene blue–DNA) $= 2.13 \times 10^4\ M^{-1}$ for methylene blue–DNA, K(acridine orange–DNA) $= 2.69 \times 10^4\ M^{-1}$ for acridine orange and K(ethidium bromide–DNA) $= 6.58 \times 10^4\ M^{-1}$ for ethidium bromide–DNA complexes. A larger K value is estimated for ethidium bromide–DNA, because ethidium bromide provides greater accessibility for DNA binding rather than methylene blue and acridine orange. Similar association constants were reported for DNA complexes with different drugs [54–57].

3.7. Macrocalorimetry

3.7.1. Thermodynamics and stability of pigment–DNA-adducts

The data obtained from isothermal titration microcalorimetry of DNA interaction with ligand are shown in Fig. 5. Fig. 5a shows the heat of each injection and Fig. 5b shows the heat related to each total concentration of ligand. To obtain the dissociation equilibrium constant (K_d) and the molar enthalpy of binding (ΔH), a simple graphical fitting method is used for calorimetric data analysis according to the equation [58–62]:

$$\Delta H = 1/A_i\{(B_i + K_d) - [(B_i + K_d)_2 - C_i]^{1/2}\} \qquad (1)$$

where

$$A_i = V_i/2Q_i$$

$$B_i = [\text{DNA}]_{\text{total}} + [\text{Ligand}]_{\text{total}}$$

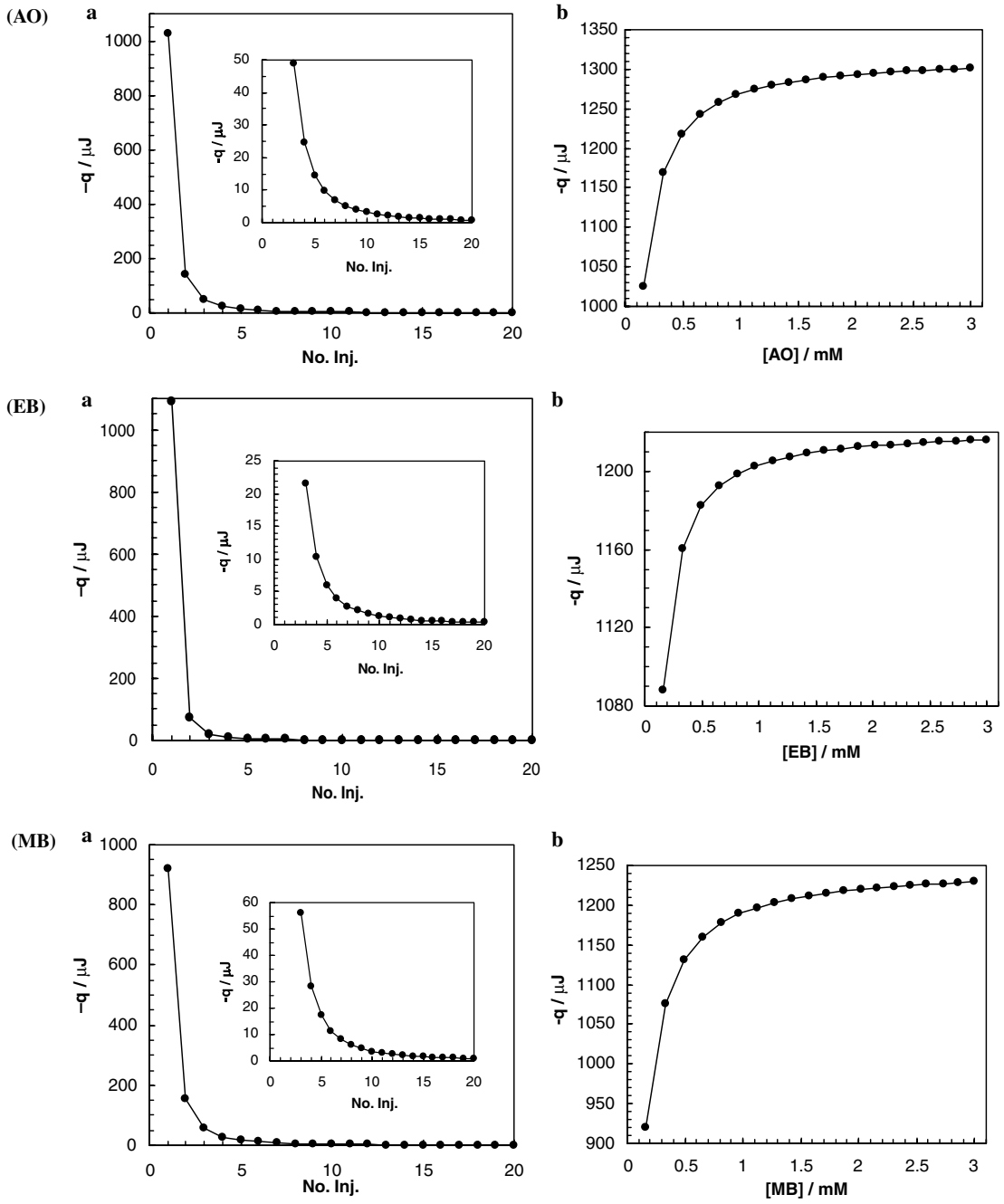

Fig. 5. (a) The heat of ligand binding on DNA for 20 automatic cumulative injections, each of 10 μl, of ligand solution 30 mM, into the sample cell containing 1.8 ml DNA solution at a concentration of 50 μM at pH 7.0 and 27 °C. In the inset, heat values of the first and second injections (which they are large values respect to the other injections) have not been shown to justify heat values of other injections are not zero. (b) The cumulative heat of ligand binding related to each total concentration of ligand, calculated from Fig. 1A.

$$C_i = 4[\mathrm{DNA}]_{\mathrm{total}}[\mathrm{Ligand}]_{\mathrm{total}}$$

where V_i is the volume of the reaction solution in the sample cell and Q_i is heat of interaction in each titration step. So, A_i, B_i and C_i are known in each titration process. Therefore, Eq. (1) contains two unknown parameters, K_d and ΔH. A series of reasonable values for K_d is inserted into Eq. (1) and corresponding values for ΔH are calculated and the graph ΔH versus K_d is constructed. Curves of all titration steps will intersect in one point, which represents the true value for ΔH and K_d.

The plots of ΔH versus K, according to Eq. (1), for first 10 injections, are shown in Fig. 6. The intersection of curves gives:

$\{\mathrm{EB}\}$ $K_d = 15\mu\mathrm{M}$ $\Delta H = -13.58$ kJ/mol
$\{\mathrm{AO}\}$ $K_d = 36\mu\mathrm{M}$ $\Delta H = -14.63$ kJ/mol
$\{\mathrm{MB}\}$ $K_d = 46\mu\mathrm{M}$ $\Delta H = -13.87$ kJ/mol

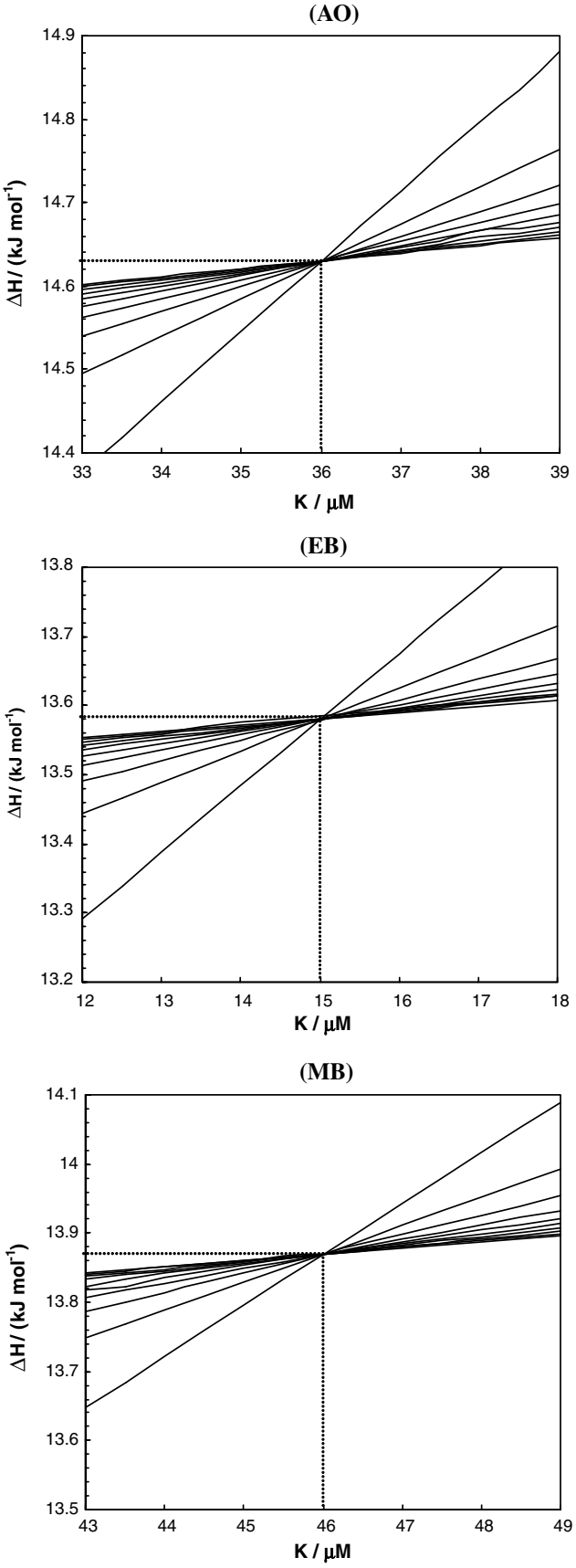

Fig. 6. ΔH versus K for the first 10 injections in the reasonable values of K_d, according to Eq. (1) and data from Fig. 5b. The coordinates of intersection point of curves give true value for ΔH and K_d.

The conformity of dissociation binding constants (K_d) obtained from microcalorimetric and spectrophotometric studies (UV) is observed.

On the basis of our spectroscopic and microcalorimeric results the intercalation and external binding of MB, AO and EB to DNA duplex have been concluded with the order of overall binding constants $K_{EB} = 6.58 \times 10^4\ M^{-1} > K_{AO} = 2.69 \times 10^4\ M^{-1} > K_{MB} = 2.13 \times 10^4\ M^{-1}$ and dissociation constants of $K_{EB} = 15\ \mu M > K_{AO} = 36\ \mu M > K_{MB} = 46\ \mu M$. The pigment interaction induced a partial B-DNA to A-DNA conformational transition.

Acknowledgments

The financial support of the Natural Sciences and Engineering Research Council of Canada (NSERC), FCAR (Quebec), Azad University, Central Tehran Branch and Research Council of University of Tehran is gratefully acknowledged.

References

[1] D. Pastre, O. Pietrement, A. Zozime, E. Le Cam, Biopolymers 77 (2005) 53–62.
[2] M.R. Bugs, M.L. Cornelio, Photochem. Photobiol. 74 (2001) 512–520.
[3] N.W. Luedtke, Q. Liu, Y. Tor, Chem. Eur. J. 11 (2004) 498–508.
[4] M.J. Warning, J. Mol. Biol. 13 (1965) 269–282.
[5] J.B. Le Pecq, C. Paoletti, J. Mol. Biol. 27 (1967) 87–106.
[6] R.J. Douthart, J.P. Burnett, F.W. Beasley, B.H. Frank, Biochemistry 12 (1973) 214–220.
[7] C.C. Tsai, S.C. Jain, H.M. Sobell, J. Mol. Biol. 114 (1977) 301–315.
[8] J.L. Bresloff, D.M. Crothers, Biochemistry 20 (1981) 3547–3553.
[9] V.W.F. Burns, Biochem. Biophys. 133 (1969) 420–424.
[10] Ph.J. Wahl, C. Paoletti, J.-B. Le Pecq, Proc. Natl. Acad. Sci. USA 65 (1970) 417–421.
[11] J. Olmsted III, D.R. Kearns, Biochemistry 16 (1970) 3647–3654.
[12] D.P. Heller, C.L. Greenstock, Biophys. Chem. 50 (1994) 305–312.
[13] J. McCann, N.E. Spingarn, J. Kobori, B.N. Ames, Proc. Natl. Acad. Sci. USA 72 (1975) 979–983.
[14] M.J. Warning, Annu. Rev. Biochem. 50 (1981) 159–192.
[15] H. Nishiwaki, M. Miura, R. Ohno, K. Kawashima, Cancer Res. 34 (1974) 2699–2703.
[16] B.R. Balda, G.D. Birkmayer, Yale Biol. Med. 46 (1973) 464–470.
[17] R.V. Guntaka, B.W. Mahy, J.M. Bishop, H.E. Varmus, Nature 253 (1975) 507–511.
[18] N.W. Luedke, Y. Tor, Biopolymers 70 (2003) 103–119.
[19] M.J. Warring, J. Mol. Biol. 13 (1965) 269–282.
[20] J.B. Lepecq, C. Paoletti, J. Mol. Biol. 27 (1967) 87–106.
[21] V.D. Vacquier, J. Brachet, Nature 222 (1969) 193–195.
[22] N.W. Luedke, Q. Liu, Y. Tor, Bioorg. Med. Chem. 11 (2003) 5235–5247.
[23] S.C. Jain, C.C. Tasi, H.M. Sobell, J. Mol. Biol. 114 (1977) 317–331.
[24] C. Medhi, J.B. Mitchel, S.L. Price, A.B. Tabor, Biopolymers 52 (1999) 84–93.
[25] D. Reha, M. Kabelac, F. Ryjacek, J.E. Sponer, M. Elstner, S. Suhai, P. Hobza, J. Am. Chem. Soc. 124 (2002) 3366–3376.
[26] C.A. Hunter, K.R. Lawson, J. Perkins, C.J. Urch, J. Chem. Soc. Perkin Trans. 2 (2001) 651–669.
[27] J. Sponer, J. Leszczynski, P. Hobza, Biopolymers 61 (2001) 3–31.
[28] S.E. Patterson, J.M. Coxon, L. Strekowski, Bioorg. Med. Chem. 5 (1997) 277–281.
[29] P.U. Giacomoni, M. Le Bert, FEBS Lett. 29 (1973) 227–230.

[30] F. Cozzi, M. Cinquini, R. Annuziata, J.S. Siegel, J. Am. Chem. Soc. 115 (1993) 5330–5331.
[31] R. Rohs, H. Sklenar, J. Biomol. Struct. Dyn. 21 (2004) 699–711.
[32] G. Laustrait, Biochemie 68 (1986) 771–778.
[33] E.M. Tuite, B. Norden, J. Am. Chem. Soc. 116 (1994) 7548–7556.
[34] W. Muller, D.M. Crothers, Eur. J. Biochem. 54 (1975) 267–277.
[35] C. Ohuigin, D.J. McConnell, J.M. Kelly, W.J.M. Van der Putten, Nucleic Acids Res. 45 (1987) 167–175.
[36] E.M. Tuite, J.M. Kelley, Biopolymers 35 (1995) 419–433.
[37] J.M. Kelley, W.J.M. Van der Putten, D. McConnell, J. Photochem. Photobiol. 45 (1987) 167–175.
[38] W.J.M. Van der Putten, J.M. Kelley, Photochem. Photobiol. 49 (1989) 145–151.
[39] S. Alex, P. Dupuis, Inorg. Chim. Acta 157 (1989) 271–281.
[40] J.F. Neault, H.A. Tajmir Riahi, J. Phys. Chem. B 102 (1998) 1610–1614.
[41] J.F. Neault, H.A. Tajmir Riahi, J. Biol. Chem. 271 (1996) 8140–8143.
[42] A. Ahmed-Ouameur, H.A. Tajmir-Riahi, J. Biol. Chem. 279 (2004) 42041–42054.
[43] Sh. Nafisi, A. Sobhanmanesh, K. Alimoghaddam, A. Ghavamzadeh, H.A. Tajmir-Riahi, DNA Cell Biol. 24 (2005) 634–640.
[44] Sh. Nafisi, M. Esm-Hesseini, A. Sobhanmanesh, H.A. Tajmir-Riahi, J. Mol. Struct. 750 (2005) 23–28.
[45] Sh. Nafisi, A. Hadji Akhoondi, A.R. Yektadoost, Biopolymers 74 (2004) 345–351.
[46] E. Thaillanier, J. Liquier, Methods Enzymol. 211 (1992) 307–335.
[47] G.I. Dovbeshko, V.I. Chegel, N.Y. Gridna, O.P. Shishov, Y.M. Tryndiak, V.P. Todor, G.I. Solyanik, Biopolymers (Biospectroscopy) 67 (2002) 470–486.
[48] D.M. Loprette, K.A. Hartmann, Biochemistry 32 (1998) 4077–4082..
[49] J. Stephanos, J. Inorg. Biochem. 62 (1996) 155–162.
[50] W. Zhong, Y. Wang, J.S. Yu, Y. Liang, K. Ni, S. Tu, J. Pharm. Sci. 93 (2004) 1039–1046.
[51] A. Ahmed Ouameur, R. Marty, H.A. Tajmir-Riahi, Biopolymers 77 (2005) 129–135.
[52] M.I. Klotz, L. Hunston, Biochemistry 10 (1982) 3065–3069.
[53] M. Purcell, A. Novetta-Delen, H. Arakawa, H. Malonga, H.A. Tajmir-Riahi, J. Biomol. Struct. Dyn. 17 (1999) 473–480.
[54] V.V. Andrushchenko, Z. Leonenko, H. Van de Sande, H. Wieser, Biopolymers 61 (2002) 243–260.
[55] A.M. Polyanichko, V.V. Andrushchenko, E.V. Chikhirzhina, V.I. Vorobev, H. Wieser, Nucleic Acid Res. 32 (2004) 989–1002.
[56] R. Marty, A. Ahmed Ouameur, J.F. Neault, Sh. Nafisi, H.A. Tajmir-Riahi, DNA Cell Biol. 23 (2004) 135–140.
[57] H.A. Tajmir-Riahi, J.F. Neault, M. Naoui, S. Diamatoglou, Biopolymers 35 (1996) 493–501.
[58] M. Mhadermarzi, A.A. Saboury, A.A. Moosavi-Movahedi, Pol. J. Chem. 72 (1998) 2024–2028.
[59] A.A. Saboury, F. Karbassi, Thermochim. Acta 362 (2000) 121–129.
[60] A.A. Saboury, A. Divsalar, G. Ataie, A.A. Moosavi-Movahedi, M.R. Housaindokht, G.H.J. Hakimelahi, Biochem. Mol. Biol. 35 (2002) 302.
[61] N.S. Sarraf, A.A. Saboury, A.A. Moosavi-Movahedi, J. Enzyme Inhib. Med. Chem. 17 (2002) 203–206.
[62] A.A. Saboury, J. Therm. Anal. Cal. 72 (2003) 93–103.